

2 Nanoparticle-Based Drug Delivery for Hemodynamic

3 Disruption in Idealized Aneurysmal Arteries

12
13
14
15

ABSTRACT

Aims: Cardiovascular disease continues to pose a significant global health challenge in modern society. Aneurysmal dilation markedly modifies hemodynamic patterns, potentially leading to thrombus formation and vascular complications. Nanoparticles (NPs) represent potential agents for targeted drug delivery; however, their effects on arterial flow behavior and hemodynamic parameters necessitate additional research. This study investigates nano-therapeutic transport and its impact on blood flow characteristics in idealized aneurysmal arteries through computational fluid dynamics (CFD).

Study design: A three-dimensional computational model was created for a healthy artery (Case 1) and an aneurysmal artery (Case 2). The aneurysmal artery models featured dilation diameters of 5 mm, 8 mm, and 10 mm to examine the impact of aneurysm size on hemodynamic behavior. Comparative analyses were conducted with and without nanoparticles in pulsatile blood flow conditions.

Methodology: A pulsatile velocity profile was applied at the inlet, with a constant outlet pressure of 16,000 Pa sustained. Blood was characterized as a non-Newtonian fluid through the application of the Carreau–Yasuda model. Computational hemodynamic parameters, such as velocity magnitude, wall shear stress, oscillatory shear index, and relative residence time, were examined with and without the presence of nanoparticles. A detailed computational mesh was utilized to guarantee the numerical stability and accuracy of the simulations.

Results: The healthy artery in Case 1 had a WSS of 11.3543 Pa, while Case 2 with nanoparticles had 10.9176 Pa. As aneurysm diameter increased, WSS decreased in the sac. Due to nanoparticles, Case 2 WSS distribution was smoother than Case 1. The healthy artery and aneurysm diameters of 5 mm, 8 mm, and 10 mm had OSI values of 0.1429 with nanoparticles, while those without nanoparticles were 0.142857, 0.142804, 0.1428571, and 0.1428571. Both patients had moderate to high RRT values, indicating prolonged blood particle occupancy near the aneurysm wall. The results also showed that (1) arteries with nanoparticles had lower velocity, (2) Case 1 without nanoparticles had 3.85% higher WSS than Case 2 with nanoparticles, (3) nanoparticles produced a smoother WSS profile, and (4) prolonged residence time near the aneurysm wall may increase thrombosis risk. Local flow dynamics and hemodynamic indicators were greatly altered by aneurysmal dilatation. Nanoparticles lowered flow velocity and smoothed the WSS curve while marginally altering OSI and RRT. These findings shed light on nanoparticle-assisted medicine delivery in vascular diseases and may improve treatment methods.

Conclusion: The outcomes demonstrate the substantial influence of hemodynamic variables on the progression and remodeling of curved arteries with aneurysms, especially

when nanoparticles are present. The results of the research are

- The artery containing nanoparticles (Case 2) demonstrates a reduced velocity in comparison to the artery devoid of nanoparticles (Case 1).
- The Case -1 demonstrates a 3.85% increase in WSS relative to Case -2.
- An inverse relationship exists between aneurysm diameter and velocity in both instances.
- The RRT values in the 10 mm aneurysmal artery exceed those in the healthy artery by 99.90% in both instances.

This indicates a high-risk area, where the extended residence time of blood particles adjacent to the vessel wall may facilitate vascular remodeling.

16

17

Keywords: Nanoparticles; CHD factors; Cardiovascular-disorder; non-Newtonian; CFD

18

19

20

1. INTRODUCTION

21

22

23

24

25

26

27

28

29

30

31

32

33

34

35

36

37

38

39

40

41

42

43

44

45

46

47

48

49

50

51

52

A number of research have helped to comprehend the intricate link between artery geometry, blood rheology, and nanoparticle transport. Researchers revealed that proximal stenosis leads to more severe hemodynamic disruptions than distal stenosis, but both generate the same degree of lumen loss. This is owing to higher flow acceleration and enhanced recirculation zones around the restricted region [3]. The results emphasize the importance of lesion location in blood flow interruption and treatment delivery efficiency. Moreover, it has been shown that the size of nanoparticles is an important factor in regulating dispersion properties and drug transport efficiency in vascular systems. Smaller nanoparticles are usually more penetrative and diffusive but larger particles may suffer more inertial effects and different residence periods in aneurysmal sacs.

53 The effect of Brownian motion on the transport of nanoparticles has also been studied
54 extensively. It has been found that the random movement of nanoparticles is increased with
55 the increase of the Brownian motion parameter, which causes the enhanced particle
56 diffusion and mixing inside the blood flow field [3]. This effect is especially critical in low
57 velocity recirculation zones inside aneurysms, where increased particle dispersion may
58 result in improved targeted medication deposition. Furthermore, the study of the non-
59 Newtonian blood flow behavior showed that the fluid velocity increases with the growing of
60 the coupling stress inverse parameter, which indicates the substantial dependency of
61 hemodynamic characteristics on the rheological properties [4]-[8]. Accurate rheological
62 modeling of blood, especially in diseased arteries, is required for realistic prediction of flow
63 patterns and nanoparticle delivery, due to its shear-thinning nature.

64 Commonly accepted as essential markers of vascular disease development and thrombus
65 formation are the hemodynamic parameters of WSS, OSI and RRT. They showed that
66 increase in aneurysm diameter and magnetic field strength resulted in decrease in WSS
67 while OSI and RRT values increased at the same time [9]. Reduced WSS areas are
68 associated with endothelial dysfunction and thrombus formation whereas increased OSI and
69 RRT signify disrupted oscillatory flow and increased particle residence times near the artery
70 wall. These hemodynamic anomalies may have a considerable effect on the aggregation of
71 nanoparticles and medication delivery efficiency in the aneurysmal regions.

72 Cerebral aneurysms are a major public health problem globally. Studies have revealed that
73 about 3–5% of the global population may develop cerebral aneurysms, and nearly 1–2% of
74 these aneurysms rupture annually, sometimes leading to severe neurological problems or
75 death [10], [11]. The significant risk of aneurysm rupture drives the demand for novel
76 therapeutic techniques that could potentially improve localized treatment and reduce the
77 necessity for invasive operations. In this context, nanoparticle-based drug delivery systems
78 provide a promise for the selective targeting of sick sections of the artery wall and the
79 improvement of therapeutic accuracy.

80 In addition, studies comparing healthy, stenosed, and aneurysmal arteries have shown that
81 non-Newtonian blood modeling gives much greater values of velocity and wall shear stress
82 than Newtonian assumptions. In particular, maximal velocity increased by 7.96% and WSS
83 increased by 220.98% during systole in stenosed and aneurysmal arteries compared to
84 healthy and treated arteries [12]-[15]. These results highlight the importance of genuine non-
85 Newtonian blood behavior in CFD models to accurately anticipate the hemodynamic
86 circumstances and nanoparticle transport dynamics.

87 Furthermore, the researchers found that the variation in the fluid rheology can alter the
88 velocity, temperature and concentration distribution, and the particle absorption rates, and
89 therefore, directly affect the efficiency of drug delivery systems [16]. Such rheological effects
90 are particularly relevant in nanoparticle-mediated therapies, where variations in flow
91 behavior have a strong impact on particle deposition, residence time and therapeutic
92 dispersion within sick arteries. Previous studies generally show that nanoparticle transport in
93 aneurysmal arteries is influenced by a complicated interplay of vascular geometry, blood
94 rheology, hemodynamic factors and particle dynamics. The CFD-based studies provide
95 useful insights into these mechanisms and lead to the development of safer and more
96 effective nanoparticle-assisted treatment options for cardiovascular disorders.

97

98 **2. MATERIAL AND METHODS**

99

100 A three-dimensional computational model of healthy and aneurysmal arteries was created to
 101 study nanoparticle transport and hemodynamics using CFD. We considered 5 mm, 8 mm,
 102 and 10 mm aneurysms. The Carreau–Yasuda model modeled blood as non-Newtonian. A
 103 constant outflow pressure of 16,000 Pa and pulsatile inflow flow were used. Velocity
 104 magnitude, WSS, OSI, and RRT were simulated with and without nanoparticles. Fine
 105 computational meshes ensured numerical accuracy and solution stability.

106

107 **2.1 Governing Equations**

108

109 The blood flow within the aneurysmal artery was considered to be incompressible, laminar,
 110 and non-Newtonian. The governing equations include the continuity equation and the
 111 Navier–Stokes momentum equations. The governing equations of the research work are
 112 follows

113

$$\nabla \cdot \mathbf{u} = 0 \tag{1}$$

114

$$\frac{\partial C}{\partial t} + \mathbf{u} \cdot \nabla C = D \nabla^2 C \tag{2}$$

115

$$D = \frac{k_B T}{6\pi\mu r} \tag{3}$$

116

117 Here C is the concentration, \mathbf{u} is the velocity of blood flow, D is the diffusion coefficient
 118 of nanoparticle with radius r, k_B is the Boltzmann constant, μ is the viscosity and T is
 119 temperature.

119

The non-Newtonian Carreau-Yasuda equation is

120

$$\mu = \mu_\infty + (\mu_0 - \mu_\infty) [1 + (\lambda \dot{\gamma})^a]^{\frac{n-1}{a}} \tag{4}$$

121

where a and $\lambda > 0$, the shear rate of blood flow is explained by $\dot{\gamma} = \sqrt{2S:S}$

122

$$\text{where } S = \frac{1}{2} [\nabla \mathbf{u} + (\nabla \mathbf{u})^T] \tag{5}$$

123

124 Here μ is the apparent viscosity, λ is the relaxation time, μ_0 is the zero shear rate
 125 viscosity, μ_∞ is the infinite shear rate viscosity, n is the power index and a is the transition
 126 parameter. In this study the following simulation parameters are used $D = 4.86 \times 10^{-12}$
 127 $[m^2/s]$, $k_B = 1.38 \times 10^{-23} \text{ m}^2\text{kg}/(\text{s}^2 \cdot \text{K})$, $\mu = 0.0035 \text{ [Pa}\cdot\text{s]}$, $r = 40 \text{ [nm]}$, $\mu_0 = 0.03568 \text{ [Pa}\cdot\text{s]}$,
 128 $\mu_\infty = 0.035 \text{ [Pa}\cdot\text{s]}$, $a = 2$, $\lambda = 8.1313 \text{ [s]}$, $n = 1.5$, $\rho = 1060 \text{ [kg}\cdot\text{m}^{-3}]$ and $T = 310 \text{ [K]}$.that more
 129 precisely represent the rheology of blood than considering a constant viscosity.

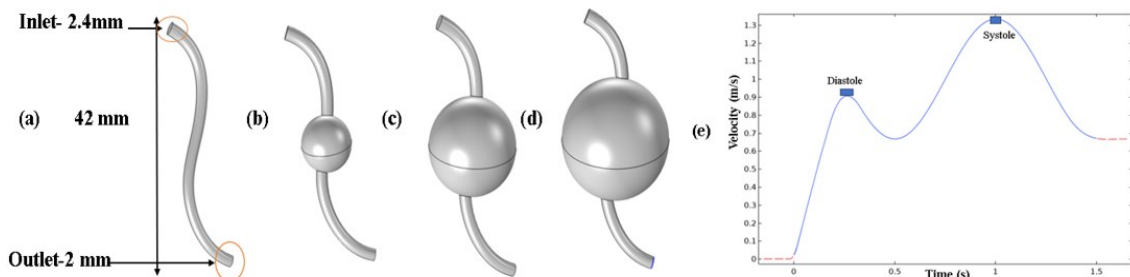
129

130 **2.2 Physical Model**

131

132 This study uses free CAD software to make 3D models of curving arteries. The segmented
 133 data is utilized to construct idealized 3D models featuring aneurysms of varying dimensions.
 134 To replicate various stages of aneurysm development, the study analyzes a model free of
 135 aneurysms (healthy), along with models featuring aneurysm dimensions of 5 mm, 8 mm, and
 136 10 mm, as illustrated in Fig. 1. The boundary conditions included a pulsatile velocity profile
 137 at the intake to replicate physiological blood flow, a constant pressure or zero-gradient
 138 output, and no-slip artery walls.

138



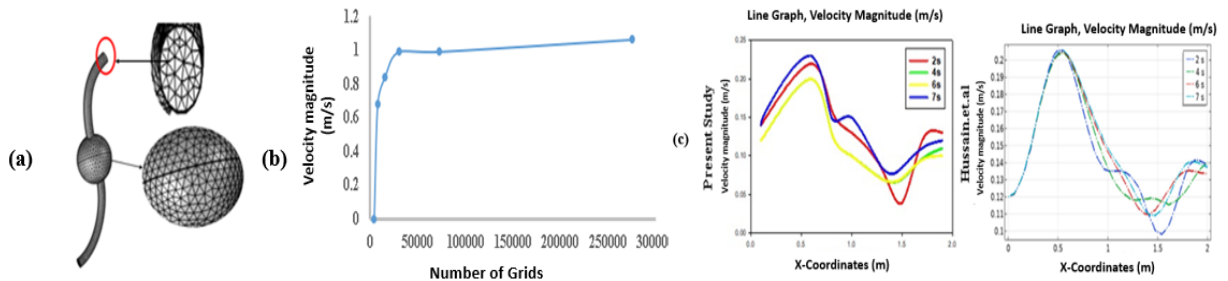
139

140 Figure 1. a) a healthy, b), c) and d) are the 5 mm, 8 mm, 10 mm aneurysmal arteries
 141 respectively, e) pulsatile flow profile

142 The variation in aneurysm size facilitates the examination of hemodynamic variables
 143 across multiple geometric shapes. Figure 1 illustrates the models in 1(a–d). Each artery in
 144 Fig. 1 presents the idealized artery model was created with aneurysms of varying diameters.
 145 The single stenosis models, each of which has a 0% area of stenosis in the artery, are
 146 illustrated in Figure 1 (b-d). The models are shown in Figure 1. (a–d). Case-1 represents the
 147 artery without nanoparticles, while Case-2 represents the artery with nanoparticles
 148

149 **2.3 Appropriate Grid and Boundary Conditions**

150
 151 A pulsatile flow waveform is implemented at the inlet boundary to accurately simulate
 152 physiological blood flow conditions throughout the cardiac cycle, while a constant outlet
 153 pressure of 15,600 Pa is set at the outlet boundary. The specified boundary conditions
 154 facilitate precise predictions of transient hemodynamic behavior in the aneurysmal artery. To
 155 enhance numerical accuracy and stability in CFD simulations, a fine mesh configuration is
 156 utilized across the computational domain. The mesh is refined in proximity to the arterial wall
 157 and aneurysmal sac to accurately capture critical gradients in velocity, pressure, and
 158 WSS. The numerical model employed in this study is validated against the results published
 159 by Hussain et al. [17], demonstrating strong agreement and confirming the reliability and
 160 accuracy of the computational methodology. The simulation results indicate that aneurysm
 161 geometry and local flow characteristics have a significant impact on nanoparticle transport
 162 and dispersion behavior. Proximal regions of the aneurysm demonstrate increased
 163 nanoparticle accumulation, attributed to disturbed flow recirculation and extended particle
 164 residence time. A suitable computational grid, as depicted in Fig. 2(a), is established to
 165 effectively resolve blood flow dynamics and nanoparticle transport within the artery. A grid
 166 independence analysis is conducted by progressively refining the computational mesh until
 167 minimal variations in hemodynamic parameters are detected [18]. The grid independence
 168 results shown in Fig. 2(b) demonstrate that the chosen mesh yields accurate and mesh-
 169 independent numerical solutions.



170

171 Figure 2. a) Mesh b) Grid test and c) Validation between present study with Hussain et.al
 172 [4].

173

TABLE 1: Material Properties

174

175

176

177

178

179

180

Material property name	Gold (Au)	Blood
Density [kg/m ³]	19300	1060
Viscosity [Pa*s]	0	0.0035
Thermal Conductivity[W/(m*K)]	317	0.5
Specific Heat[J/kg°C]	129	3600

181 Table 1 above illustrates the various material characteristics of nanoparticles and blood.

182

183

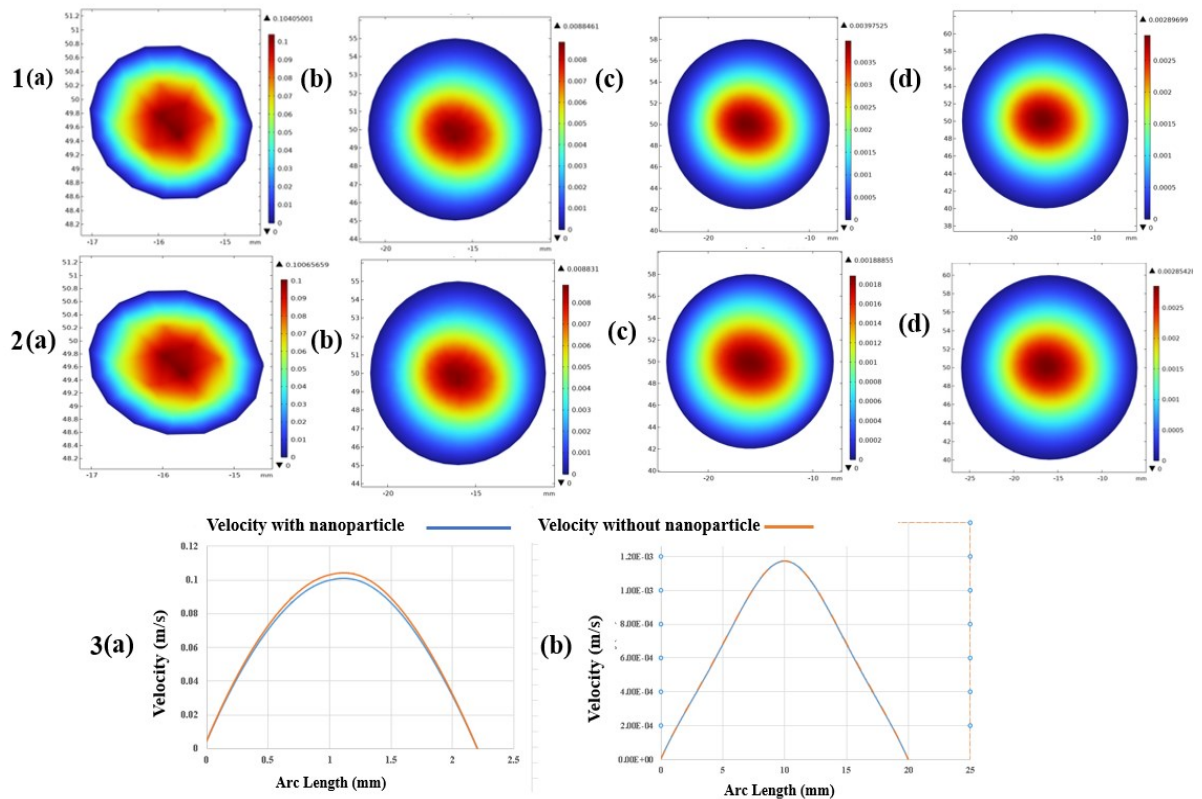
184 **3. RESULTS AND DISCUSSION**

185

186 The findings indicate that the shape of aneurysms and the presence of nanoparticles
187 significantly influence blood flow dynamics. Nanoparticles reduce flow intensity, while a
188 decrease in aneurysm diameter results in lower velocity. Healthy arteries exhibited greater
189 WSS compared to aneurysmal regions, with Case-1 consistently demonstrating higher WSS
190 than Case-2. OSI remains largely stable, suggesting minor flow oscillations across all
191 models. A longer RRT in larger aneurysms indicates an increased risk of thrombosis and
192 vascular remodeling. Nanoparticles modify wall shear stress and decrease velocity, thereby
193 influencing localized drug delivery and arterial flow. Figures 3 and 4 display the
194 computational results derived from the non-Newtonian Carreau–Yasuda blood flow model
195 utilized in this research. The figures illustrate the impact of aneurysmal dilation and
196 nanoparticle incorporation on velocity distribution and WSS characteristics in the arterial
197 domain.

198 Figure 3 presents the velocity contours along with the associated velocity profiles for two
199 distinct cases. Figures 3.1(a–d) illustrate the velocity contours for a healthy artery and
200 aneurysmal arteries with dilation diameters of 5 mm, 8 mm, and 10 mm, respectively,
201 excluding nanoparticles. Figures 3.2(a–d) illustrate the same arterial configurations with the
202 incorporation of nanoparticles into the blood flow. Figures 3.3(a–b) present the
203 corresponding velocity graphs, facilitating a quantitative comparison between the two cases.
204 Figures 3.1(a) and 3.2(a), representing healthy artery models, demonstrate the highest
205 velocity magnitudes, attributed to the lack of aneurysmal enlargement and diminished flow
206 disturbance. The velocity depicted in Figure 3.1(a) is approximately 3.85% greater than that
207 presented in Figure 3.2(a). This reduction suggests that the incorporation of nanoparticles
208 elevates the effective resistance in the bloodstream, consequently resulting in a minor
209 decrease in flow velocity within the healthy artery. Nanoparticles influence the rheological
210 properties of fluids and enhance momentum dissipation.

211 The velocity within the aneurysmal sac region decreases markedly in both instances due to
212 the abrupt expansion of the arterial lumen, leading to flow deceleration and recirculation. The
213 velocity profiles presented in Figure 3.3(b) indicate that the flow behavior within the
214 aneurysm is largely consistent across both cases, with the nanoparticle-laden flow displaying
215 marginally reduced velocity values. Moreover, an increase in aneurysm diameter from 5 mm
216 to 10 mm leads to a systematic decrease in velocity magnitude. Larger aneurysms produce
217 wider recirculation zones and diminished core flow, leading to extended particle residence
218 time and altered hemodynamic conditions.



219

220 Figure 3. Velocity contours 1(a-d) (without nanoparticle) and 2(a-d) (with nanoparticle), 3(a-b)

221 show velocity graph.

222 Figure 4 illustrates the contours of WSS for the four arterial models, accompanied by their

223 respective graphical representations. Wall shear stress is an important hemodynamic

224 parameter linked to endothelial function, vascular remodeling, and thrombus formation.

225 Figure 4.1(a) presents the WSS distribution for the healthy artery in Case 1, with a maximum

226 WSS value of 11.3543 Pa noted. Figure 4.2(a), representing the healthy artery with

227 nanoparticles (Case 2), indicates a marginally reduced WSS value of 10.9176 Pa. The

228 reduction in WSS further substantiates the role of nanoparticles in diminishing flow intensity

229 and smoothing velocity gradients adjacent to the arterial wall. In the region of the

230 aneurysmal sac, wall shear stress significantly decreases in both scenarios as the diameter

231 of the aneurysm increases. The expansion of the arterial cavity diminishes the near-wall

232 velocity gradient, resulting in decreased shear stress values along the aneurysm wall.

233 Regions of low WSS are significant due to their strong correlation with endothelial

234 dysfunction, blood stagnation, and thrombus formation. The results indicate that larger

235 aneurysms generate more adverse hemodynamic conditions.

236 Figure 4.3(a) illustrates that the WSS profile for Case 2 exhibits greater smoothness and

237 uniformity in comparison to Case 1. The smoother behavior results from nanoparticles,

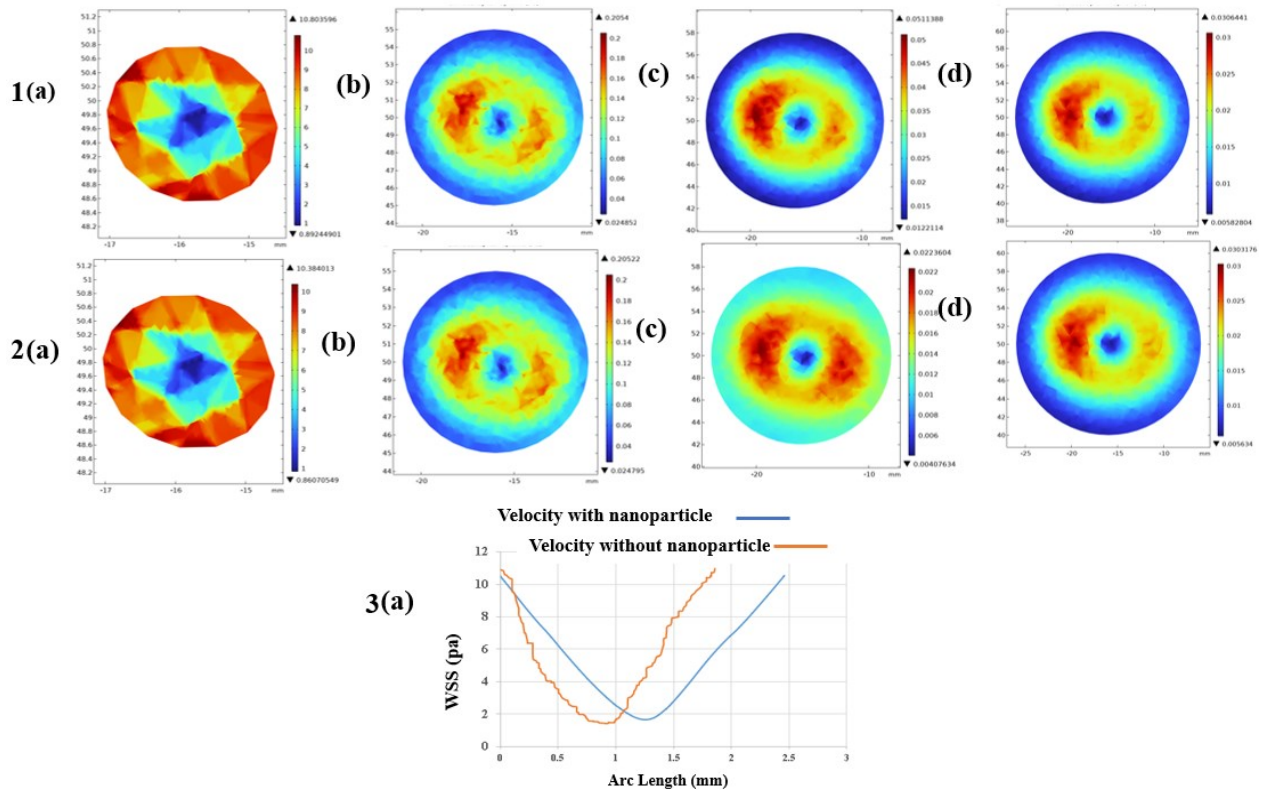
238 which alter flow characteristics and diminish abrupt changes in shear stress distribution. The

239 incorporation of nanoparticles in flow dynamics seems to stabilize local hemodynamic

240 fluctuations and result in a more gradual variation of wall shear stress along the arterial wall.

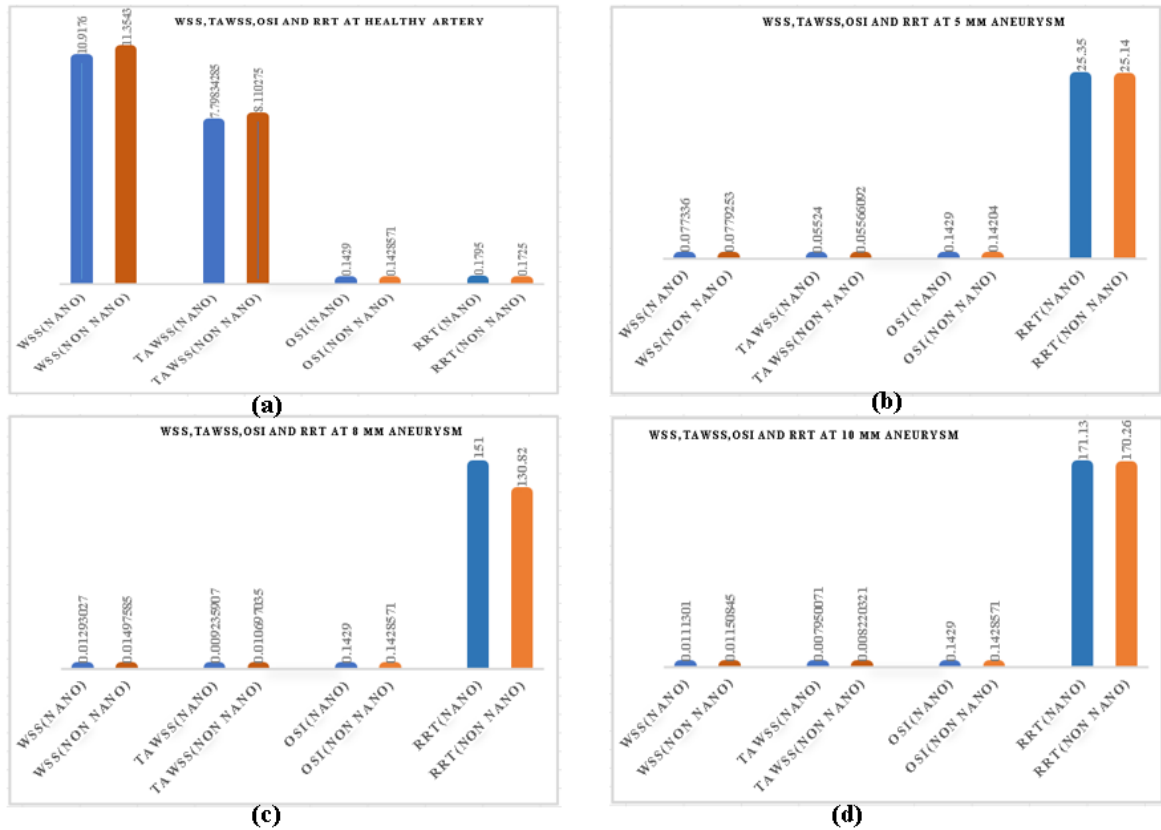
241 The findings indicate that the incorporation of nanoparticles can affect both therapeutic

242 transport and the overall hemodynamic environment in aneurysmal arteries.



243
244
245

Figure 4. WSS contours 1(a-d) (without nanoparticle) and 2(a-d) (with nanoparticle) ,3(a) shows WSS graph.



246 Figure 5. WSS, TAWSS, OSI and RRT values for a) a healthy, b), c) and d) are the 5 mm, 8
 247 mm, 10 mm aneurysmal arteries

248 Figure 5 presents a detailed comparison of hemodynamic parameters, specifically WSS,
 249 OSI, and RRT, across all arterial models examined in this study. The comparison illustrates
 250 the impact of aneurysmal dilation and nanoparticle incorporation on local blood flow
 251 dynamics and vascular wall conditions. The WSS analysis indicates that wall shear stress
 252 values are consistently elevated in Case-1 (without nanoparticles) compared to Case-2 (with
 253 nanoparticles) across all arterial configurations. In the healthy artery model, the WSS value
 254 is recorded as 11.354 Pa in Case 1, while Case 2 shows a marginally lower value of 10.918
 255 Pa. The observed reduction in WSS suggests that nanoparticles alter the rheological
 256 properties of blood flow, leading to a decrease in the near-wall velocity gradient. The
 257 nanoparticles enhance momentum dissipation and facilitate a more uniform hemodynamic
 258 environment within the artery. In aneurysmal artery models with diameters of 5 mm,
 259 and 10 mm, the WSS values significantly decrease in both scenarios compared to the
 260 healthy artery. The enlarged aneurysmal sac induces flow deceleration and the development
 261 of recirculation zones, which markedly decrease the shear stress exerted on the arterial wall.
 262 In the 5 mm aneurysm model, the WSS value in Case-1 is approximately 0.76% greater than
 263 in Case-2. The 8 mm aneurysm model demonstrates a 13.66% increase in WSS in Case-1
 264 compared to Case-2, whereas the 10 mm aneurysm model shows a 3.29% rise in WSS for
 265 Case-1 relative to Case-2. The findings demonstrate that the incorporation of nanoparticles
 266 consistently reduces wall shear stress across the arterial system. A clear inverse relationship

267 exists between aneurysm diameter and wall shear stress in both instances. With an increase
268 in aneurysm diameter from 5 mm to 10 mm, there is a progressive decrease in WSS values.
269 Larger aneurysmal expansions lead to broader flow separation and recirculation zones,
270 which in turn result in diminished near-wall flow velocity gradients. The decrease in WSS
271 holds clinical significance, as low WSS is closely linked to endothelial dysfunction, vascular
272 inflammation, and atherogenic mechanisms. Regions subjected to consistently low WSS
273 exhibit increased vulnerability to pathological vascular remodeling, potentially facilitating the
274 onset of thrombosis and the formation of atherosclerotic plaques. Figure 5 presents the
275 distributions of the OSI for all models. The OSI values in Case-1 exhibit minor variations
276 between healthy and aneurysmal arteries; nonetheless, all values consistently approximate
277 0.1429 in both scenarios. The comparable OSI values suggest that the incorporation of
278 nanoparticles does not significantly affect the oscillatory characteristics of pulsatile blood
279 flow. An OSI value of approximately 0.1429 indicates a moderate level of shear stress
280 oscillation, suggesting that the flow experiences only mild directional fluctuations. Moderate
281 oscillatory shear can contribute to endothelial cell dysfunction, particularly when it occurs
282 alongside low wall shear stress and extended blood residence times. Combined
283 hemodynamic conditions can expedite vascular wall degeneration and the progression of
284 disease in aneurysmal regions.

285 The analysis of RRT underscores the altered flow conditions within the aneurysmal arteries.
286 The RRT values for the healthy artery model are 0.1795 in Case-1 and 0.1725 in Case-2.
287 The values are considerably below the established critical threshold of 1, suggesting
288 physiologically stable flow conditions and a low risk of pathological particle accumulation.
289 The low RRT values indicate that blood particles do not persist near the vessel wall for
290 prolonged durations in a healthy artery. The 8 mm aneurysm model demonstrates the most
291 significant difference in RRT between Case-1 and Case-2, suggesting that this intermediate
292 size may be especially responsive to flow disturbances and nanoparticle influences. The
293 other aneurysmal models exhibit persistently high RRT values that surpass the critical
294 threshold of 1. Elevated RRT values suggest the existence of significantly disturbed flow
295 regions, where blood particles remain in close proximity to the arterial wall for extended
296 periods. RRT values between 35 and 171 indicate moderate to high-risk hemodynamic
297 zones linked to endothelial dysfunction, vascular remodeling, inflammatory responses, and
298 the onset of plaque formation. Extended residence time promotes greater interaction
299 between blood components and the arterial wall, consequently increasing the risk of
300 thrombosis and pathological alterations within the aneurysm. The findings indicate that
301 aneurysmal enlargement significantly alters local flow dynamics and generates adverse
302 hemodynamic conditions, potentially facilitating disease progression and vascular
303 complications.

304 **4. CONCLUSION**

305

306 The results demonstrate the hemodynamic variables affect the evolution, remodeling, and
307 pathological behavior of curved aneurysmal arteries, especially when nanoparticles are
308 added to the blood flow. Varying velocity distribution, WSS, and RRT greatly impact the local
309 vascular environment and may cause endothelial dysfunction, thrombosis, and aneurysm
310 growth. Nanoparticles affect artery flow and hemodynamic response. The simulation findings
311 show that Case-2's artery has lower velocity magnitudes than Case-1's. Nanoparticles

312 increase effective flow resistance and change blood rheology, reducing velocity. The
313 interaction between nanoparticles and surrounding fluid particles increases circulatory
314 momentum dissipation. Thus, Case-2 flow is smoother and less explosive. The aneurysmal
315 sac's increased artery geometry already slows and recirculates flow, reducing velocity. The
316 analysis shows that Case-1 has 3.85% higher WSS than Case-2. This decrease in WSS
317 suggests that nanoparticles diminish the near-wall velocity gradient and smooth the artery
318 wall shear stress distribution. WSS directly affects endothelial cell activity and vascular
319 health, hence such reductions may affect artery biology. Lower WSS areas often have flow
320 disturbances, endothelial dysfunction, inflammation, and thrombus development. Thus,
321 nanoparticle-induced WSS decrease may affect vascular wall remodeling. Both cases show
322 an inverse association between aneurysm diameter and blood flow velocity. Velocity
323 decreases with aneurysm dilatation. This happens because the increased aneurysmal cavity
324 suddenly enlarges the flow domain, reducing axial momentum and creating huge
325 recirculation zones. Larger aneurysms cause slower and more disrupted flow patterns than
326 smaller ones or healthy arteries. The reduced velocity inside the aneurysm sac enhances
327 particle stagnation and blood retention near the artery wall. RRT research shows how
328 hemodynamics is disrupted in big aneurysmal arteries. The RRT values in the 10 mm
329 aneurysmal artery are 99.90% greater than those in the healthy artery in both situations. A
330 large increase in RRT implies a high-risk hemodynamic zone with prolonged blood particle
331 residence near the artery wall. High RRT values stimulate blood constituent-endothelium
332 contact, which can produce inflammatory reactions, platelet aggregation, thrombus
333 formation, and vascular remodeling. Thus, aneurysm geometry and nanoparticle integration
334 greatly affect local hemodynamic behavior and may influence vascular disease development
335 and nanoparticle-assisted treatment options.

345 **COMPETING INTERESTS**

346

347 The authors declare that there are no competing interests related to this study.

348

365 **DATA AVAILABILITY STATEMENT**

366

367 Data are available on reasonable request. All data are accessible from the corresponding
368 author upon request.

369

370 **REFERENCES**

371

372 [1] K. E. Hoque, M. Ferdows, S. Sawall, E. E. Tzirtzilakis, and M. A. Xenos,
373 “Numerical investigation of nanoparticle transport in physiological flow,” *Phys.*
374 *Fluids*, vol. 33, no. 12, p. 121907, 2021.

375 [2] M. N. Uddin, K. E. Hoque, and M. M. Billah, “Thermal and hemodynamic
376 behavior of nanofluid flow in biological systems,” *Heliyon*, vol. 10, p. e28872, 2024.

377 [3] S. S. Ardahaie, A. J. Amiri, A. Amouei, K. Hosseinzadeh, and D. D. Ganji,
378 “Modeling of nanoparticle transport in blood flow with Brownian motion effects,”
379 *Informatics Med. Unlocked*, vol. 10, pp. 71–81, 2018.

380 [4] M. Ferdows *et al.*, “Non-Newtonian blood flow analysis in stenosed arteries with
381 hemodynamic effects,” *Comput. Methods Biomech. Biomed. Eng.*, vol. 26, pp. 235–
382 248, 2023.

383 [5] R. E. Noor, K. E. Hoque, M. M. Billah, and S. Subah, “Magneto-hemodynamic
384 nanoparticle transport in arterial flow,” *Int. J. Thermofluids*, vol. 28, p. 101306,
385 2025.

- 386 [6] T. Inagawa, “Natural history of unruptured cerebral aneurysms: A comprehensive
387 review,” *Neurosurg. Rev.*, vol. 45, no. 4, pp. 2565–2582, 2022, doi: 10.1007/s10143-
388 022-01783-7.
- 389 [7] K. E. Hoque, M. M. Billah, M. S. Alam, and R. E. Noor, “Role of wall shear
390 hemodynamic characteristics in determining cerebral aneurysms severity: A stroke-
391 related study,” *Results in Engineering*, vol. 29, p. 109596, Feb. 2026, doi:
392 10.1016/j.rineng.2026.109596.
- 393 [8] M. M. Billah, K. E. Hoque, U. Habiba, and T. K. Paul, “Impact of hemodynamic
394 factors on medical image-based cardiovascular disease prediction,” *Progress in*
395 *Engineering Science*, vol. 3, no. 1, p. 100195, Dec. 2025, doi:
396 10.1016/j.pes.2025.100195.
- 397 [9] M. Sara, M. M. Billah, K. E. Hoque, N. F. Ifraj, M. S. Hossain, and S. M. A.
398 Hoq, “Computational analysis of hemodynamic parameters in coronary arteries:
399 Effects of stenosis and bifurcation angle,” *JOURNAL OF MECHANICAL*
400 *ENGINEERING AND SCIENCES*, pp. 10908–10922, Dec. 2025, doi:
401 10.15282/jmes.19.4.2025.7.0855.
- 402 [10] H. E. Salman, B. Ramazanli, M. M. Yavuz, and H. C. Yalcin, “Hemodynamic
403 factors in cerebral aneurysm formation and rupture risk,” *Front. Bioeng. Biotechnol.*,
404 vol. 7, p. 111, 2019, doi: 10.3389/fbioe.2019.00111.
- 405 [11] S. Subah, M. M. Billah, M. N. Uddin, and K. E. Hoque, “Non-Newtonian
406 modeling of blood flow in stenosed and aneurysmal arteries,” *Int. J. Thermofluids*,
407 vol. 29, p. 101367, 2025.
- 408 [12] B.I. Chowdhury, M. M. Billah, Muhammad Sajjad Hossain, S. Shifat Ahmed,
409 K. E. Hoque, Unsteady mixed convective effect in a lid driven porous t-shaped
410 cavity using nanofluid, *Numerical Heat Transfer, Part B : Fundamentals* (Taylor &
411 Francis), 2024. <https://doi.org/10.1080/10407790.2025.2532111>
- 412 [13] U.K. Suma, M. Masum Billah, Aminur Rahman Khan, K. E. Hoque,
413 Magnetohydrodynamic mixed convective heat transfer augmentation in a rectangular
414 lid-driven enclosure with a circular hollow cylinder utilizing nanofluids,
415 *International Journal of Thermofluids*, Vol. 25 (2025) 101014, pp 1-15, 2024.
- 416 [14] M. N. Uddin, K. E. Hoque, M. M. Billah, “The Impact of Multiple Stenosis and
417 Aneurysms on Arterial Diseases: A Cardiovascular Study” *Heliyon*, Vol. 10, no.
418 5(e26889), 2024, pp. 1-26.

419 [15] N. Zaman, M. Ferdows, M. A. Xenos, K. E. Hoque & E. E. Tzirtzilakis, “Effect
420 of Angle Bifurcation and Stenosis in Coronary Arteries: An Idealized Model Study.”
421 *BioMed Res. J.*, Vol. 4, No. 2, pp. 220–234, August 09, 2020.

422 [16] R. Choudhari *et al.*, “Effect of rheological parameters on nanoparticle-based
423 drug delivery in blood flow,” *Results Eng.*, vol. 21, p. 101842, 2024.

424 [17] A. Hussain, M. N. Riaz Dar, and E. M. Tag-eldin, “CFD analysis of aneurysmal
425 blood flow with hemodynamic validation,” *Heliyon*, vol. 9, no. 7, 2023.

426 [18] K. E. Hoque, S. Sawall, M. A. Hoque, and M. S. Hossain, “Hemodynamic
427 Simulations to Identify Irregularities in Coronary Artery Models,” *J. Adv. Math.*
428 *Comput. Sci.*, vol. 28, no. 5, pp. 1–19, 2018.
429 <https://doi.org/10.9734/JAMCS/2018/43598>

430

431